Fibroblast response is enhanced by poly(L-lactic acid) nanotopography edge density and proximity

Keith R Milner[1]
Christopher A Siedlecki[1,2]

Departments of Surgery[1] and Bioengineering[2], Pennsylvania State University College of Medicine, Hershey, PA, USA

Abstract: The development of scaffolds for use in tissue engineering applications requires careful choice of macroscale properties, such as mechanical characteristics, porosity and biodegradation. The micro- and nano-scale properties of the scaffold surface are also an important design criterion as these influence cell adhesion, proliferation, and differentiation. The cellular response is known to be affected by surface topography but the mechanisms governing this remain unclear. Homogenous poly(L-lactic acid) was textured with surface nanotopographies by two-stage replication molding of heterogeneous demixed polymer films. Initial cell adhesion was improved on nanotextured surfaces compared with smooth controls, but subsequent cell density was significantly reduced on the roughest surfaces. Improvements in cell response were found to correlate with focal contact and actin microfilament development. Cell response was found to trend both with the surface density of topography edges and with inter-topography spacing, indicating possible roles for edges stimulating cell adhesion/proliferation or for spacing to modulate the ability of integrin-ligand bonds to cluster and form focal adhesions. This study furthers understanding of the geometric properties of surface nanotopographies that affect cellular response. It is hoped that identification of the mechanisms governing cell-topography interactions will allow rule-based design of biomaterial surface to engineer specific cellular responses.
Keywords: nanotopography, replication, biomaterials, cell adhesion, roughness

Introduction

There is great interest in the development of scaffolds suitable for use in tissue engineering and regenerative medicine. An appropriate scaffold would have mechanical properties matching those of the desired tissue, porosity optimized for cell response and flow transport, and biodegradation and resorption matched to tissue growth rate (Hutmacher 2000). In addition to these bulk, macro-properties of the scaffold, the scaffold surface properties would be designed to encourage cell adhesion, proliferation, and differentiation. Such micro- and nanoscale properties include surface chemistry, topography, and biological activity.

Numerous studies have implicated a role for surface nanotopography affecting the cell response, with both increased and decreased adhesion reported (Vance et al 2004; Wan et al 2005). It has been proposed that nanoscale roughness affects cell adhesion as a bell curve trend, with surfaces having high or low roughness showing reduced cell density compared with surfaces having an optimum roughness (Fan et al 2002), however the mechanisms that govern this response remain unclear. It has been hypothesized that protein adsorption or conformational changes preferentially occur at surface discontinuities. This has been suggested as a mechanism for the so-called contact alignment phenomenon experienced by cells seeded on parallel ridges (Curtis and Wilkinson 1997), where focal adhesions have been observed to preferentially

Correspondence: Keith R Milner
The Pennsylvania State University,
The Milton S. Hershey Medical Center,
Biomedical Engineering Institute,
Department of Surgery, H151, 500
University Drive, Hershey, PA 17033, USA
Tel +1 717 531 6130
Fax +1 717 531 4464
Email kmilner@psu.edu

form on the edges and sidewalls of such features (Uttayarat et al 2005). Furthermore, the adhesive force between cell and substrate has been shown to increase with increasing number of ridges per unit area (and therefore increasing edge density) (Karuri et al 2004). It has also been demonstrated that cell binding site availability was increased in vitronectin adsorbed on nanostructured PLGA compared with microstructured or smooth samples (Miller et al 2005). However, it should be noted that contact alignment is also observed on ridges fabricated without sharp discontinuities (Walboomers et al 1999), suggesting the presence of additional mechanisms influencing the cellular response, which may include direct mechanotransduction (Dalby et al 2004b) and geometric constraint (Milner and Siedlecki 2007).

Cell adhesion to a biomaterial surface is a key requirement to cell survival, since non-adherent cells will apoptose via anoikis (Frisch and Francis 1994). Cell adhesion to adsorbed proteins is often mediated by integrin receptor binding, with initial receptor-ligand bonds forming submicron sized focal complexes located primarily in the leading lamella of cells and subsequently clustering and maturing in to larger focal adhesions (Zaidel-Bar et al 2003). The mature focal adhesions transmit force and tension between the cell and adsorbed proteins, maintaining cell adhesion, and act as nexuses for signaling pathways governing subsequent events such as proliferation and differentiation (Sastry and Burridge 2000). Surface topography may therefore be key in determining cellular response by modulating focal complex formation and maturation, by affecting protein adsorption and conformation or by affecting the ability of integrins to cluster.

Surface topography may be created using a number of techniques ranging from lithographic micro- and nanofabrication to produce ordered features to chemical etching, electrospinning and colloidal lithography for random distributions (Norman and Desai 2006). Polymer demixing is receiving attention as a rapid method for fabricating surface nanotopographies. A two polymer mixture is spin cast so that phase separation occurs, resulting in topographies distributed across the surface with geometry determined by choice of polymers, solvent, substrate and spin casting parameters (Affrossman et al 1996; Heriot and Jones 2005), with cell response shown to vary with topography geometry (Dalby et al 2003b; Lim et al 2005). There have been a number of reports examining cellular response to nanotopographies formed by spin casting mixtures of polystyrene (PS) and poly(4-bromostyrene) (PBrS) (Dalby et al 2002a, 2004a). In this PS/PBrS system, the resulting surface topography consists of PBrS islands within a sea of PS (Affrossman et al 1996). It is therefore common to anneal the substrates above the glass transition temperature of PS, to allow the PS to migrate and reduce surface chemistry heterogeneity. Thereafter Br is not found within 10 Å of the surface but is located within 70 Å of the surface (Dalby et al 2003a).

The objective of this study was to examine the response of human fibroblasts to demixed polymer nanotopographies created on the surface of a homogenous, biomedically relevant polymer. Surface nanotopography was formed by phase separating polymers of limited biomedical applicability (PS and PBrS) on glass substrates. A two-stage replication molding technique (Milner et al 2006) was then used to recreate these nanotopographies on to the surface of poly(L-lactic acid) films.

Materials and methods

Poly(L-lactic acid) substrates

A two-stage replication molding process based on soft lithography was used to replicate demixed polymer nanotopographies on to the surface of poly(L-lactic acid) films (PLLA). Briefly, demixed polymer nanotopographies were prepared via the spin casting technique described by Affrossman using a mixture of PS and PBrS (Affrossman et al 1996). Elastomeric molds were fabricated by casting poly(dimethylsiloxane) (PDMS) over the demixed polymer master topographies. PLLA was then cast in to the molds, replicating the original two-polymer master nanotopographies in to a homogeneous material.

Master topographies were prepared from polymer blends with w/w ratio of 40% PS (M_W = 240,000) to 60% PBrS (M_W = 65,000) (both Sigma-Aldrich, St Louis, MO). These were dissolved in toluene at total polymer concentrations of 5%, 2% and 0.5% w/w. Glass coverslips of 25 mm dia. were cleaned by sonication in chloroform and then by glow discharge plasma (ambient atmosphere, 100 W; Harrick Scientific Products, Pleasantville, NY). A 50 µl aliquot of polymer blend was spin cast on to a coverslip for 60 sec at 4000 rpm (P6700 Spincoater, Specialty Coating Systems, Indianapolis, IN). During spin casting it is thought that the polymer film thins through removal of solution, stratifies in to two layers, thins via solvent evaporation leading to destabilization of the polymer interface, and the polymers then phase separate laterally (Heriot and Jones 2005), creating surface topography of PBrS islands within a sea of PS. Smooth control surfaces were fabricated by spin casting 5% PS in toluene on to coverslips.

Elastomeric negatives of the master topographies were created in Sylgard 184 PDMS (Dow Corning, Midland, MI). This was mixed at 10:1 base:curing agent, degassed to remove bubbles, poured over the PS/PBrS to a depth of ~10 mm, degassed again, cured at 65 °C for 4 hr and peeled gently from the PS/PBrS. Replicas of the master topographies were created in PLLA (MW = 50,000; Polysciences, Warrington, PA). This was dissolved in chloroform at 2% w/v, 400 μl was aliquoted on to a PDMS mold and a cleaned, 12 mm dia. glass coverslip was placed on top of the PLLA solution. The chloroform was allowed to evaporate at room temperature and the coverslip was removed from the silicone, now coated with a PLLA film having surface topography replicating that of the PS/PBrS masters. The PLLA films were then placed in an oven at 45 °C under 29" Hg vacuum overnight. The 12 mm coverslip was used to provide rigidity and mass to the sample, facilitating handling and ensuring samples remained submerged during cell culture.

Surface topographies were assessed via atomic force microscopy (AFM) under ambient conditions using a Digital Instruments Nanoscope III Multimode AFM (Veeco Instruments, Santa Barbara, CA). Images were acquired in tapping mode using probes with long, narrow tips grown by electron beam deposition to minimize tip enlargement artifacts (STING probes; MikroMasch, Wilsonville, OR). Images were analyzed via the standard Digital Instruments AFM software and also via ImageJ image analysis software following extraction as jpeg files (free download from National Institutes of Health: http://rsd.info.nih.gov/ij/).

Cell culture

Normal human, telomerase negative fibroblasts derived from the foreskin (CRL-2522, American Type Culture Collection, Manassas, VA) were cultured in minimum essential medium containing Earle's salts and 0.1 mM nonessential amino acids supplemented with 2 mM L-glutamine, 100 U/ml penicillin-streptomycin and 10% fetal bovine serum (all Invitrogen, Carlsbad, CA). PLLA substrates were sterilized by exposure to UV light for 2 hr and fibroblasts were then seeded at a density of 1×10^4 cells/ml in 2 ml of culture medium per well of a 12-well tissue culture polystyrene plate (Becton Dickinson, Franklin Lakes, NJ). Samples were incubated at 37 °C in 5% CO_2 atmosphere with the medium replaced every 2–3 days. Fibroblasts were chosen as the model cell since their roles in wound repair and extra-cellular matrix deposition make them ideal candidates for engineering tissue, such as skin, bone and blood vessels (Wang et al 2003; Choong et al 2006; L'Heureux et al 2006), and in order to enable comparisons with the works of Dalby and colleagues (2004a) examining cell response to heterogeneous PS/PBrS demixed polymer film nanotopographies.

Assessment of cellular response

Fibroblast density and confluence were assessed at post-seeding times of 20 min, 3 hr, 1 day, 3 days, and 7 days. Nonadherent cells were removed by washing with phosphate-buffered saline (PBS) and adherent cells were fixed with 4% paraformaldehyde in PBS (PFA). Adherent cells were stained with SimplyBlue SafeStain (Invitrogen). Digital images of adherent cells were recorded by phase contrast microscopy (Optiphot 3; Nikon, Melville, NY). A minimum of three areas was assessed on each of three samples for each PLLA surface texture and smooth control. Experiments were performed for a total of 5 replicates. The number of adherent fibroblasts and total confluence was assessed for each digital image via ImageJ.

Cytoskeletal analysis

Focal contact formation and actin microfilament development were assessed by immunofluorescent microscopy (Optiphot 3; Nikon). Nonadherent cells were removed by washing with 37 °C PBS and adherent cells were then fixed with 37 °C PFA for 30 min. Focal contacts were immunofluorescently labeled using monoclonal mouse anti-vinculin IgG_1 primary antibody (Sigma-Aldrich) and Alexa Fluor 488 conjugated goat anti-mouse IgG_1 secondary antibody (Molecular Probes, c/o Invitrogen). Actin microfilaments were then labeled with Alexa Fluor 568 conjugated phalloidin (Molecular Probes). Permeabilization was performed using 0.05% saponin (Fluka, c/o Sigma-Aldrich) and non-specific reactions were blocked by 3% normal goat serum (Jackson Immuno, West Grove, PA).

Scanning electron microscopy

Fibroblast morphology and interaction with the PLLA surfaces were assessed by scanning electron microscopy (SEM). Samples were rinsed in 0.2 M sodium cacodylate buffer (SCB: Electron Microscopy Sciences, Hatfield, PA) and fixed with 2.5% glutaraldehyde in SCB. Samples were dehydrated by sequential immersion in 20%, 50%, 60%, 70%, 80%, 90% and 100% ethanol dilutions, air dried, sputter coating with a 10 nm gold film and imaging with a Philips XL-20 SEM.

Statistical analysis

Statistical analyses were performed via nonparametric ANOVA (Kruskal-Wallis test) using InStat (GraphPad

Software, San Diego, CA). This nonparametric test was used in preference to a standard ANOVA since the variances of the data sets did not demonstrate equality, a required assumption of the standard ANOVA. Means of experimental data were compared and differences were considered statistically significant for $p < 0.05$. Significant differences are denoted in the figures of this report using one symbol for $p < 0.05$, two for $p < 0.01$ and three for $p < 0.001$.

Results and discussion

PLLA surface topography

AFM measurements of the PS/PBrS demixed polymer films spin cast on to glass coverslips demonstrated the formation of surface nanotopographies (Figure 1a–c), comparable with that reported elsewhere (Dalby et al 2002a). These nanotopographies were then translated in to a homogenous, biomedically-relevant polymer using a previously evaluated two-stage replication molding technique (Miller et al 2004; Milner et al 2006). Replication molded PLLA films were assessed by AFM, and demonstrated surface nanotopography comparable with the PS/PBrS masters (Figure 1d–f). These surfaces are shown to scale in Figure 1g.

Geometric characteristics of the PLLA topographies are reported in Table 1. Surface roughness (R_{rms}), change in sample area relative to sample footprint, and height of the topographic features were determined via Digital Instruments AFM software. ImageJ software was used to assess mean area occupied by individual elevated features, effective feature radius (calculated from area assuming circular geometry), center-center spacing (calculated from topography centroids), inter-topography spacing (calculated from center-center spacing and radii) and edge density (total topography perimeter length normalized to sample footprint area). These are comparable to those reported elsewhere (Dalby et al 2002b, 2003a). The nanotopographies created from 5% PS/PBrS demonstrated a bimodal distribution, with large islands having mean height and diameter of 126 nm and ~4 μm respectively interspersed among smaller islands having mean height and diameter of 84 nm and ~800 nm. A number of trends were observed as total polymer concentration decreased from 5% to 0.5% PS/PBrS in toluene. Firstly, topography size (height, area, and effective radius) and inter-topography spacing decreased. Secondly, sample surface area decreased. It should be noted that surface area change was small, with the greatest change being only 1.1% in PLLA replicated from 5% masters. Given the roughly cylindrical nature of the nanotopographies, the majority of the surface area change may be ascribed to the sidewalls of the features. Thirdly, topography edge density increased with decreasing polymer concentration.

Fibroblast response to PLLA topographies

Cell confluence was assessed for post-seeding times up to 7 days. Cell density was assessed up to 3 days, with the 7 day data omitted due to the difficulty of discriminating individual cells at this time point. Results are presented in Figure 2 both as raw data in the upper panels and with data normalized to respective smooth replicates in the lower panels. Cell density and confluence at low time points was greater on textured PLLA than on smooth controls, significantly so on 2% and 0.5% samples at 3 hr and on 2% samples at 20 min. At later time points, cell density and confluence were comparable on smooth 2% and 0.5% samples. However, density and confluence on the 5% samples was significantly lower than on all other samples at 3 and 7 days.

These experiments using homogeneous PLLA nanotopographies compare well with results reported using heterogeneous PS/PBrS demixed polymer surfaces. Fibroblasts seeded on 5% PS/PBrS surfaces demonstrated stronger initial interactions with the surface than cells on smooth controls (Dalby et al 2003a). However, after 3 days this trend was reversed and cells on smooth substrates reaching confluence prior to those on the topographies. Fibroblasts on the PLLA surface replicated from 5% masters tended to have increased initial adhesion but as time progressed cell density and confluence were inferior to that observed on smooth PLLA, indicating reduced adhesion/proliferation and/or increased cell death on these 5% surfaces. Fibroblasts on 2% PS/PBrS surfaces demonstrated response comparable to those on smooth control after 3 days (Dalby et al 2002a). On the PLLA substrates, a significant increase in adhesion is noted on 2% compared with smooth. At later time points, the response is comparable indicting similar adhesion/proliferation/death on smooth and 2% samples. Fibroblasts on 0.5% PS/PBrS surfaces demonstrated increased proliferation after 1.8 days, increased cytoskeletal development after 3 days and gene upregulation, particularly for cell signaling, proliferation, and cytoskeleton (Dalby et al 2002a, 2002b). On the PLLA substrates in this study, fibroblast adhesion was increased compared with smooth controls, however no significant increase in long-term response was noted, with comparable cell density and confluence observed after 3 and 7 days.

These data fit with the bell-curve response proposed for the affect of surface roughness on cell density (Fan et al 2002). As surface roughness of these PLLA samples

decreased, improved cell response was found, with the 0.5% and 2% surfaces showing increased initial cell density and confluence and comparable later cell density and confluence compared with smooth controls and the rougher 5% surfaces demonstrating significantly reduced cell density and confluence at later time points. Cell response was also observed to increase with edge density. It is possible that this may be due to preferential protein adsorption or conformational changes occurring at surface discontinuities, as has been hypothesized by others.

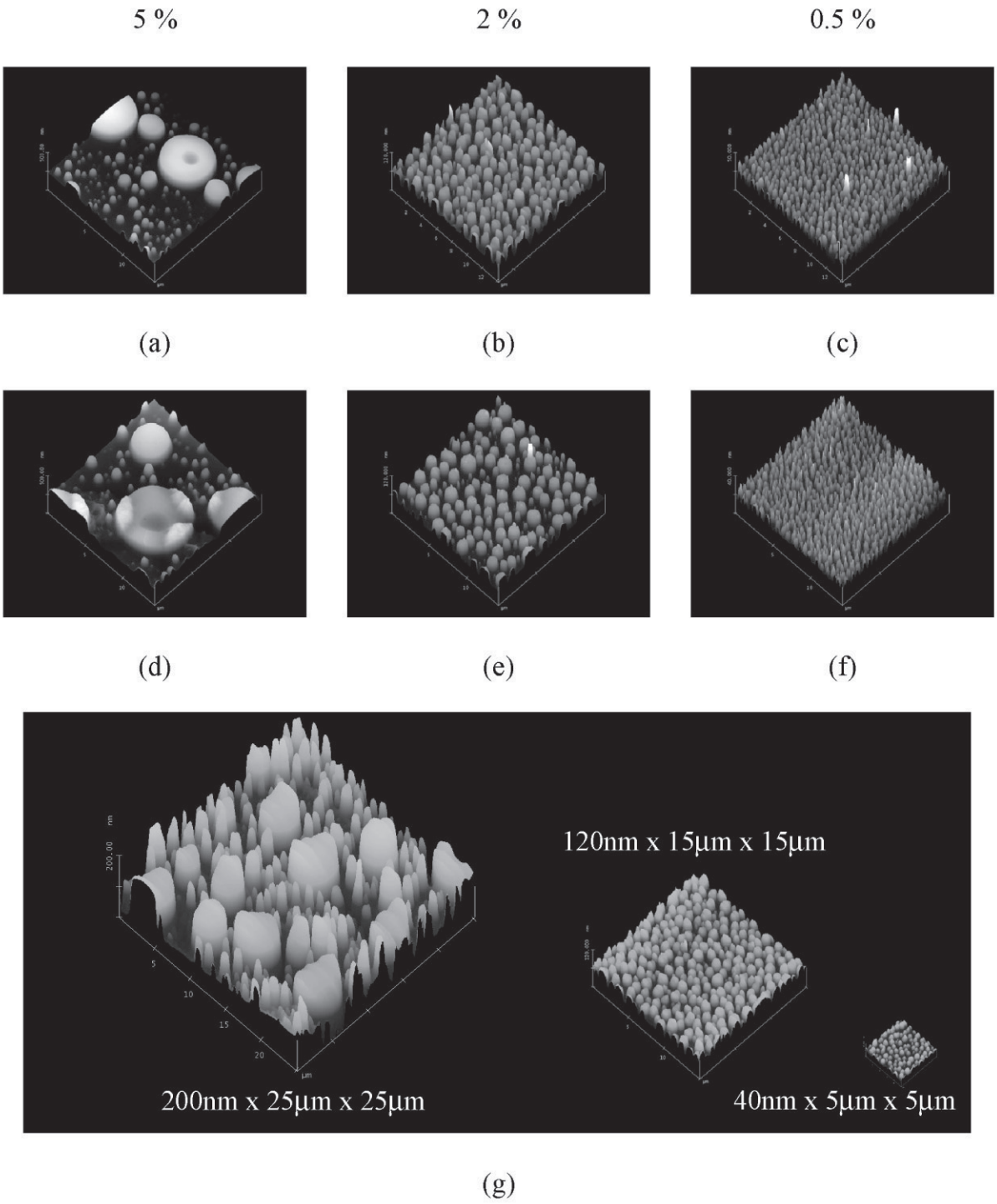

Figure 1 Atomic force microscope measurement of surface topography. Surface topography of chemically heterogeneous (**a**) 5%, (**b**) 2% and (**c**) 0.5% PS/PBrS masters was (**d,e,f**) replicated in to homogeneous PLLA films (15 × 15 µm scan area), which are (**g**) shown to scale with 5%, 2% and 0.5% PLLA from left to right.
Abbreviations: PBrS, poly(4-bromostyrene); PLLA, poly(L-lactic acid); PS, polystyrene.

Table 1 Geometric properties of PLLA nanotopographies replicated from 5 %, 2% and 0.5% PS/PBrS demixed polymer blends presented as mean ± standard deviation. PLLA from the bimodal 5% master are presented as mean data, data from large topographies (area ≥ 3 μm^2) and data from small topographies (area < 3 μm^2)

	R_{rms} (nm)	Δ Sample Area (%)	Height (nm)	Topography Area (μm^2)	Effective Radius (nm)	Center-Center Spacing[a] (nm)	Inter-Topography Spacing[a] (nm)	Edge Density (μm^{-1})
5%	52.2 ± 4.3	1.10 ± 0.15						0.59 ± 0.16
≥3 μm2			125.9 ± 12.7	12.8 ± 11.3	1900 ± 700	2850 ± 750	500 ± 400	
<3 μm2			83.7 ± 14.1	0.59 ± 0.37	400 ± 100	1750 ± 850	750 ± 750	
2%	11.3 ± 0.5	0.49 ± 0.03	30.9 ± 2.4	0.52 ± 0.26	400 ± 100	900 ± 175	125 ± 150	2.63 ± 0.15
0.5%	3.5 ± 0.3	0.18 ± 0.06	10.7 ± 1.4	0.12 ± 0.07	180 ± 60	470 ± 130	100 ± 90	4.77 ± 1.13

[a] Center-center and inter-topography spacing assessed between each feature its three nearest neighbors

Fibroblast cytoskeletal development

Variation in fibroblast density and confluence correlated well with development of focal adhesions and actin microfilaments. At 3 hr post-seeding, cells tended to be more spread on textured PLLA than on smooth controls (Figure 3). Vinculin was found at the lamellapodia edges, indicating initial focal complex formation at the cell periphery. Phalloidin staining was also observed in the cell periphery, with actin microfilaments forming at the nascent focal adhesions and starting to extend towards the cell centers. The increased cell adhesion measured on textured PLLA correlates well with the increase in focal complexes observed on those substrates.

At 3 days post-seeding, cytoskeletal development was poorest on 5% PLLA surfaces (Figure 4). Limited focal adhesions were observed, indicating poor maturation of the initial focal complexes, and the actin microfilaments were indistinct. Fibroblasts on smooth PLLA controls demonstrated large, well-formed focal adhesions and had well-developed actin cytoskeletons. Comparable actin results were observed in cells on 2% and 0.5% PLLA. Focal adhesions were also clearly observed on these substrates, but tended to be smaller in size but more numerous than on the control samples. The importance of cell attachment via focal adhesions for intra- and intercellular signaling is well understood (Sastry and Burridge 2000), and the decreased cell density and confluence at 3 and 7 days determined on the 5% PLLA correlates with the reduction in cell-substrate interactions observed here.

Cell-substrate interactions

The interaction between fibroblasts and PLLA surface textures was observed by SEM (Figure 5). At 3 hr post-seeding, cells on 5% surfaces were observed to primarily interact primarily with the larger topographies. This trend was also observed at the 3 day time point. Clear interaction between cells and large islands was noted, but pseudopods were typically limited to the inter-topography regions, only contacting the sidewalls of the small islands. Cells on 2% and 0.5% surfaces demonstrated interaction with surface topography at both time points, with pseudopods at 3 days observed on the islands, between the islands and at the edges of islands.

The reduced fibroblast density and confluence at 3 and 7 days on the 5% surfaces may be due to the limited interactions between cells and the topographies on these surfaces. Mature focal adhesions demonstrate size of several square microns and typically have multi-micron length. The small topographies found on the 5% surfaces therefore have insufficient size to support mature adhesions, but adhesions could form on the large islands and potentially in the

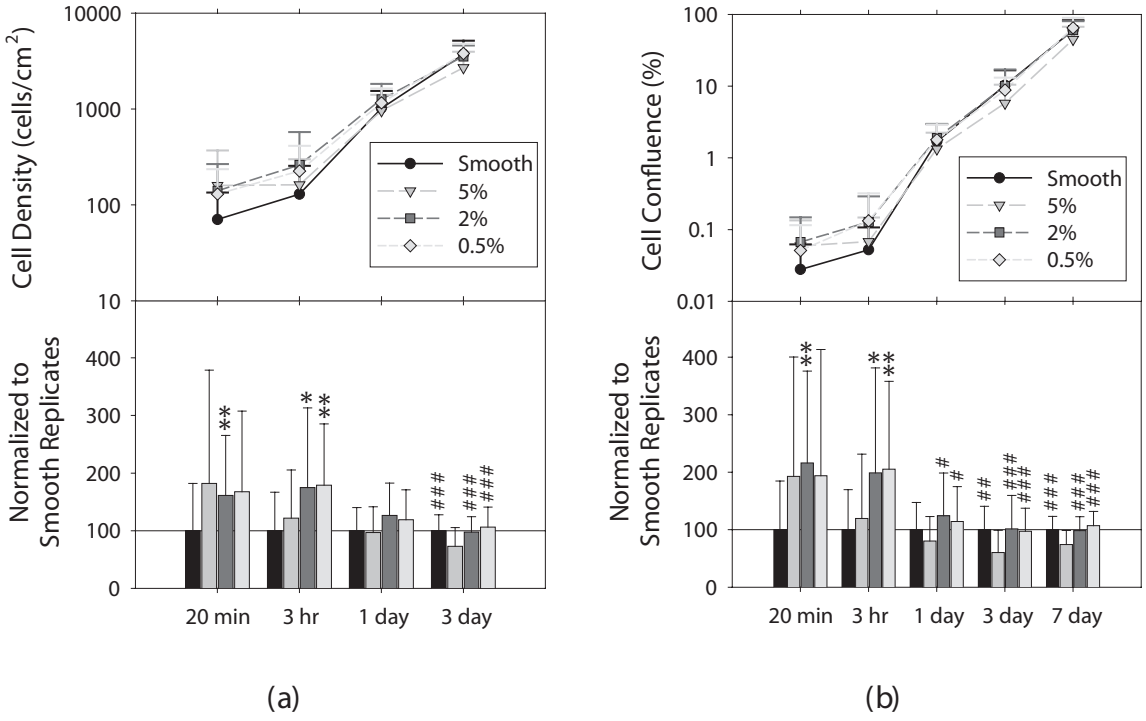

Figure 2 Fibroblast density and confluence on smooth and textured PLLA. Upper panels show mean raw data and lower panels show means of data normalized to smooth replicates for (**a**) cell density and (**b**) total confluence for post-seeding time up to 7 days with error bars denoting standard deviation (minimum over 3 areas assessed on 3 samples of each texture at each time point; 5 replicates; * and # denote statistical significance to smooth and 5% PLLA samples). Bar chart data are plotted as smooth, 5%, 2% and 0.5% from left to right at each time point.
Abbreviations: PLLA, poly(L-lactic acid).

inter-topography regions, correlating with the reduced focal adhesion development observed by fluorescent microscope and with the cell-substrate interactions observed by SEM. The topographies on 2% and 0.5% surfaces would also be of insufficient size to support whole focal adhesions. However, these features have reduced inter-topography spacing and height compared with those on the 5% surfaces. It is possible that sufficient integrin clustering may occur to allow focal adhesion formation, with adhesions either spanning topographies or forming across topographies and the intervening substrate. This may explain the reduced size but increased number of focal adhesions noted.

Conclusions

Nanotopographies were created via a polymer demixing technique, spin casting two polymers of limited biomedical relevance onto glass coverslips, and these were replicated in to homogenous poly(L-lactic acid). Surface geometric properties were observed to influence the cellular response. The topographies investigated here improved initial cell adhesion even with small changes in sample surface area. This may be due to the edge density found on the topographies. The reasons for this are unclear, but it has been hypothesized that protein adsorption or conformational changes may occur selectively at such regions. Cell density and confluence was significantly reduced on the 5% surfaces at 3 and 7 days, which had larger topographies with wider spacing. Focal adhesion maturation and cytoskeletal development was poor on these surfaces, which would be expected to alter mechanotransduction within the cells possibly leading to poor proliferation or increased cell death. Mature focal adhesions were observed on the 2% and 0.5% surfaces, although adhesions were smaller than those on smooth surfaces. This suggests that integrin clustering can occur on these surfaces, but not on the 5% surfaces where topography height and inter-topography spacing are much larger. These results demonstrate that small changes in PLLA surface area may increase initial cell adhesion, but cell proliferation remained either uniform or decreased compared with smooth controls.

Acknowledgments

This research was supported by Pennsylvania State University Department of Surgery Feasibility Grants (KRM), the Dorothy Foehr Huck and J. Lloyd Huck Institutes of the Life Sciences, the Center for Biomedical Devices and Functional Tissue Engineering, and by a grant from the

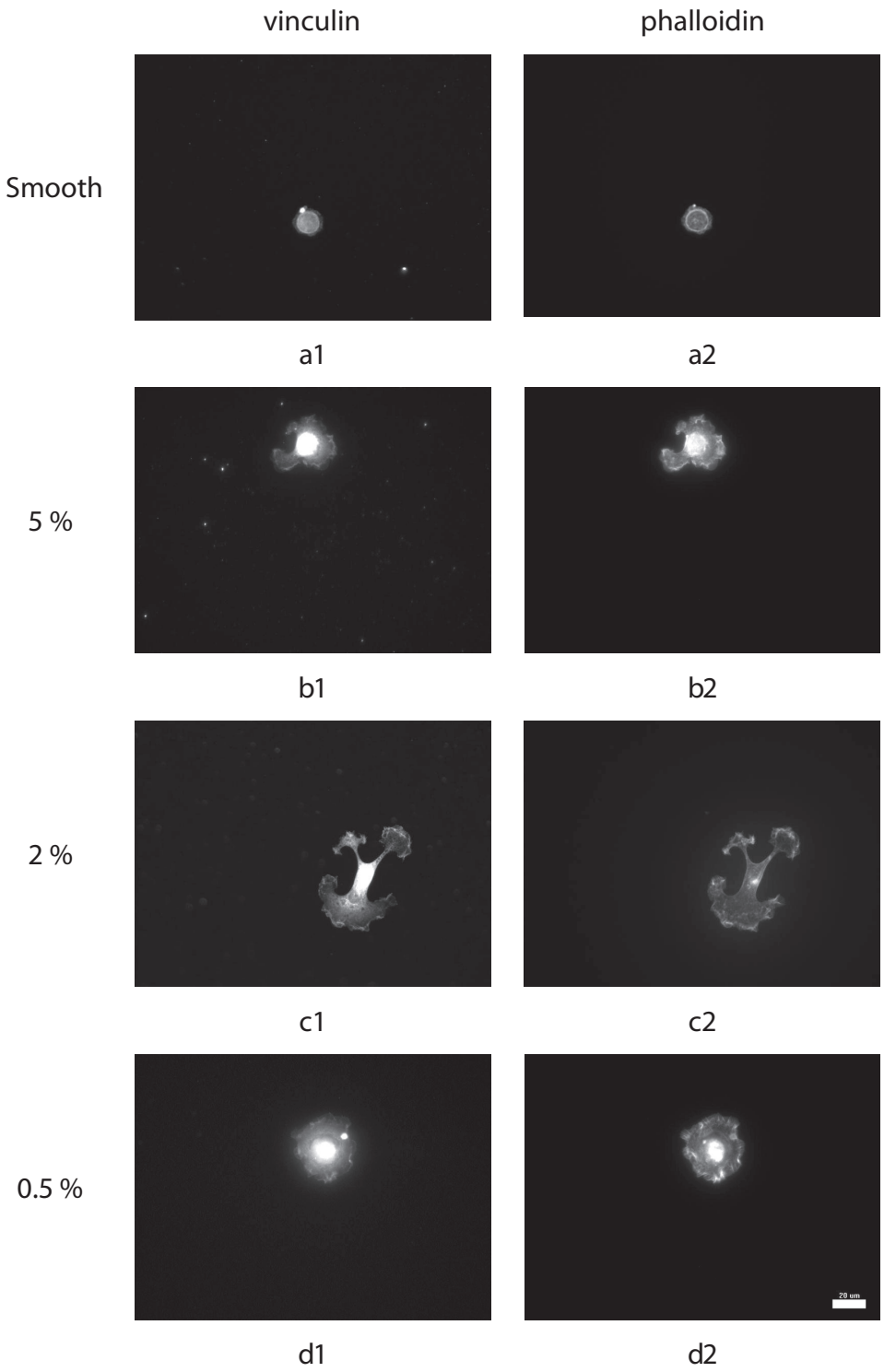

Figure 3 Representative immunofluorescent images of cytoskeletal development at 3 hour post-seeding in fibroblasts on PLLA substrates acquired with 40x objective. Focal adhesions (**1**) and actin microfilaments (**2**) in cells on PLLA replicated from (**a**) smooth, (**b**) 5%, (**c**) 2% and (**d**) 0.5% master topographies (20 μm scale bar).
Abbreviations: PLLA, poly(L-lactic acid).

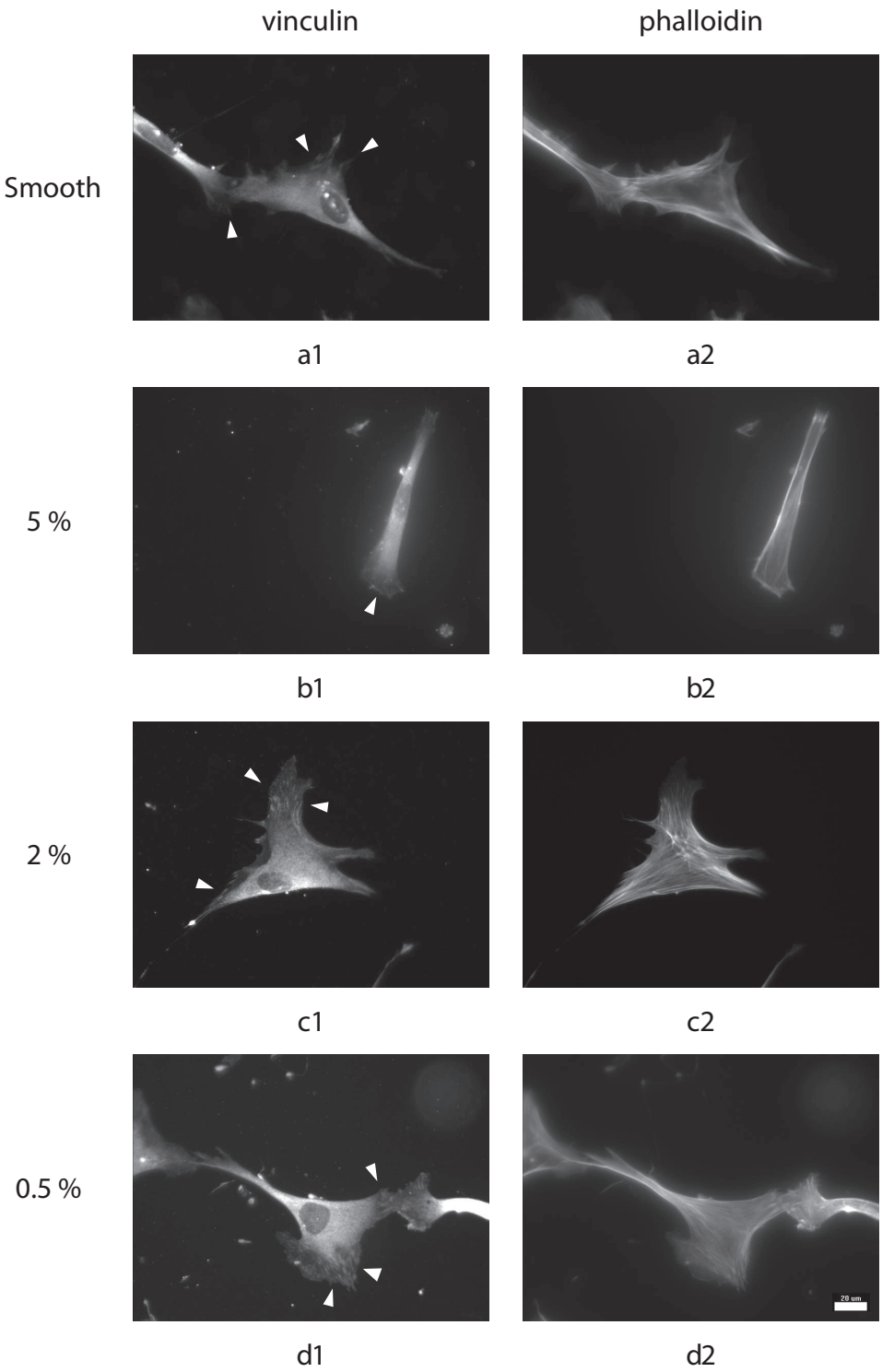

Figure 4 Representative immunofluorescent images of cytoskeletal development at 3 days post-seeding in fibroblasts on PLLA substrates acquired with 40x objective. Focal adhesions (1, indicated with arrowheads) and actin microfilaments (**2**) in cells on PLLA replicated from (**a**) smooth, (**b**) 5%, (**c**) 2%, and (**d**) 0.5% master topographies (20 μm scale bar).
Abbreviations: PLLA, poly(L-lactic acid).

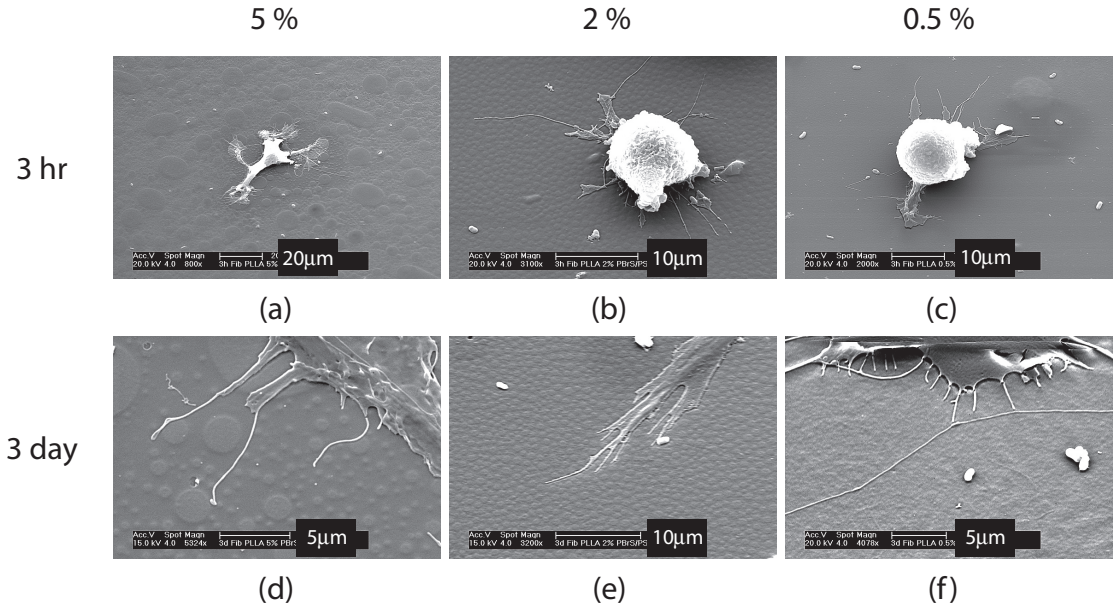

Figure 5 Scanning electron microscope images on cells on PLLA nanotopographies. Fibroblasts were observed on PLLA substrates replicated from 5%, 2%, and 0.5% master topographies after (**a,b,c**) 3 hr and (**d,e,f**) 3 days.
Abbreviations: PLLA, poly(L-lactic acid).

Pennsylvania Department of Health. The Pennsylvania Department of Health specifically disclaims responsibility for any analyses, interpretations, or conclusions. The authors gratefully acknowledge the assistance of Prof. Henry J. Donahue, Dr. Amanda Taylor, Dr. Jung Yul Lim and the Musculoskeletal Research Laboratory in the Department of Orthopaedics and Rehabilitation at the Penn State College of Medicine. We also thank Tom Rusnak and Mark Angelone at the Penn State Materials Characterization Laboratory for their assistance with SEM.

References

Affrossman S, Henn G, O'Neill SA, et al. 1996. Surface topography and composition of deuterated polystyrene-poly (bromostyrene) blends. *Macromolecules*, 29:5010–16.

Choong CSN, Hutmacher DW, Triffitt JT. 2006. Co-culture of bone marrow fibroblasts and endothelial cells on modified polycaprolactone substrates for enhanced potentials in bone tissue engineering. *Tissue Eng*, 12:2521–31.

Curtis ASG, Wilkinson CDW. 1997. Topographical control of cells. *Biomaterials*, 18:1573–83.

Dalby MJ, Childs S, Riehle MO, et al. 2003a. Fibroblast reaction to island topography: changes in cytoskeleton and morphology with time. *Biomaterials*, 24:927–35.

Dalby MJ, Giannaras D, Riehle MO, et al. 2004a. Rapid fibroblast adhesion to 27 nm high polymer demixed nano-topography. *Biomaterials*, 25:77–83.

Dalby MJ, Riehle MO, Johnstone HJH, et al. 2002a. Polymer-demixed nanotopography: Control of fibroblast spreading and proliferation. *Tissue Eng*, 8:1099–108.

Dalby MJ, Riehle MO, Johnstone HJH, et al. 2003b. Nonadhesive nanotopography: fibroblast response to poly (n-butyl methacrylate)-poly (styrene) demixed surface features. *J Biomed Mater Res A*, 67A:1025–32.

Dalby MJ, Riehle MO, Sutherland DS, et al. 2004b. Use of nanotopography to study mechanotransduction in fibroblasts – methods and perspectives. *Eur J Cell Biol*, 83:159–69.

Dalby MJ, Yarwood SJ, Riehle MO, et al. 2002b. Increasing fibroblast response to materials using nanotopography: morphological and genetic measurements of cell response to 13 nm high polymer demixed islands. *Exp Cell Res*, 276:1–9.

Fan YW, Cui FZ, Hou SP, et al. 2002. Culture of neural cells on silicon wafers with nano-scale surface topograph. *J Neurosci Methods*, 120:17–23.

Frisch SM, Francis H. 1994. Disruption of epithelial cell-matrix interactions induces apoptosis. *J Cell Biol*, 124:619–26.

Heriot SY, Jones RAL. 2005. An interfacial instability in a transient wetting layer leads to lateral phase separation in thin spin-cast polymer-blend films. *Nature Mater*, 4:782–6.

Hutmacher DW. 2000. Scaffolds in tissue engineering bone and cartilage. *Biomaterials*, 21:2529–43.

Karuri NW, Liliensiek S, Teixeira AI, et al. 2004. Biological length scale topography enhances cell-substratum adhesion of human corneal epithelial cells. *J Cell Sci*, 117:3153–64.

L'Heureux N, Dusserre N, Konig G, et al. 2006. Human tissue-engineered blood vessels for adult arterial revascularization. *Nature Med*, 12:361–5.

Lim JY, Hansen JC, Siedlecki CA, et al. 2005. Osteoblast adhesion on poly(L-lactic acid)/polystyrene demixed thin film blends: Effect of nanotopography, surface chemistry, and wettability. *Biomacromolecules*, 6:3319–27.

Miller DC, Haberstroh KM, Webster TJ. 2005. Mechanism(s) of increased vascular cell adhesion on nanostructured poly(lactic-co-glycolic acid) films. *J Biomed Mater Res A*, 73A:476–84.

Miller DC, Thapa A, Haberstroh KM, et al. 2004. Endothelial and vascular smooth muscle cell function on poly(lactic-co-glycolic acid) with nanostructured surface features. *Biomaterials*, 25:53–61.

Milner KR, Siedlecki CA. 2007. Submicron poly(L-lactic acid) pillars affect fibroblast adhesion and proliferation. *J Biomed Mater Res A*, 82A:80–91.

Milner KR, Snyder AJ Siedlecki CA. 2006. Sub-micron texturing for reducing platelet adhesion to polyurethane biomaterials. *J Biomed Mater Res A*, 76A:561–70.

Norman J, Desai T. 2006. Methods for fabrication of nanoscale topography for tissue engineering scaffolds. *Ann Biomed Eng*, 34:89–101.

Sastry SK, Burridge K. 2000. Focal adhesions: A nexus for intracellular signaling and cytoskeletal dynamics. *Exp Cell Res*, 261:25–36.

Uttayarat P, Toworfe GK, Dietrich F, et al. 2005. Topographic guidance of endothelial cells on silicone surfaces with micro- to nanogrooves: Orientation of actin filaments and focal adhesions. *J Biomed Mater Res A*, 75A:668–80.

Vance RJ, Miller DC, Thapa A, et al. 2004. Decreased fibroblast cell density on chemically degraded poly-lactic-co-glycolic acid, polyurethane, and polycaprolactone. *Biomaterials*, 25:2095–103.

Walboomers XF, Croes HJE, Ginsel LA, et al. 1999. Contact guidance of rat fibroblasts on various implant materials. *J Biomed Mater Res*, 47:204–12.

Wan YQ, Wang Y, Liu ZM, et al. 2005. Adhesion and proliferation of OCT-1 osteoblast-like cells on micro- and nano-scale topography structured poly(L-lactide). *Biomaterials*, 26:4453–9.

Wang HJ, Bertrand-De Haas M, van Blitterswijk CA, et al. 2003. Engineering of a dermal equivalent: Seeding and culturing fibroblasts in PEGT/PBT copolymer scaffolds. *Tissue Eng*, 9:909–17.

Zaidel-Bar R, Ballestrem C, Kam Z, et al. 2003. Early molecular events in the assembly of matrix adhesions at the leading edge of migrating cells. *J Cell Sci*, 116:4605–13.